

Charge Localization due to RKKY Interaction in the Spin Glass AuFe

B.Gorshunov^{1,2}, () A.S.Prokhorov², S.Kaiser¹, D.Faltermeier¹, S.Yasin¹,
M.Dumm¹, N.Drichko^{1,3}, E.S.Zhukova², I.E.Spektor², S.Vongtragool^{4,5},
M.B.S.Hesselberth⁴, J.Aarts⁴, G.J.Nieuwenhuys^{4,5}, and M.Dressel¹

¹ 1. Physikalisches Institut, Universität Stuttgart, 70550 Stuttgart, Germany

² Prokhorov General Physics Institute, Russian Academy of Sciences, Moscow, Russia

³ Io e Physico-Technical Institute, St. Petersburg, Russia

⁴ Kamerlingh Onnes Laboratory, Leiden University, Leiden, The Netherlands

⁵ Res. Department Condensed Matter, Paul Scherrer Institute, Villigen, Switzerland

PACS.75.50.Lk { Spin glasses and other random magnets.

PACS.71.55.Jv { Disordered structures; amorphous and glassy solids.

PACS.72.15.Rn { Localization effects (Anderson or weak localization).

Abstract. { Measurements of electrodynamic response of spin glass AuFe films in comparison with pure gold films are performed at frequencies from 0.3 THz (10 cm^{-1}) up to 1000 THz (33000 cm^{-1}) using different spectroscopic methods. At room temperatures the spectra of pure gold and of AuFe are typically metallic with the scattering rate of carriers in AuFe being significantly enlarged due to scattering on localized magnetic moments of Fe ions. In the spin-glass phase of AuFe at $T = 5\text{ K}$ a pseudogap in the conductivity spectrum is detected with the magnitude close to the Ruderman-Kittel-Kasuya-Yosida (RKKY) energy for AuFe: $\epsilon_{\text{RKKY}} = 2.2\text{ meV}$. The origin of the pseudogap is associated with partial localization of electrons which mediate the RKKY interaction between localized magnetic Fe centers.

Introduction. { Phenomena in spin glasses represent one of the central topics of modern solid state physics; they are of fundamental interest and also have a variety of possible applications [1]. The spin-glass state is realized in intermetallic alloys, for instance, when ions of a magnetic metal (like Fe, Mn) are introduced in small amounts into the matrix of non-magnetic noble metals (like Au, Ag, Cu, Pt). The local magnetic moments interact co-operatively with each other via the conduction electrons by the agency of the indirect Ruderman-Kittel-Kasuya-Yosida (RKKY) exchange interaction [2]. Magnitude and sign of the interaction depend on the distance between impurities. Combined with the spatial disorder this provides conditions for a spin-glass state.

Among the exceptional properties of spin glasses compared to other magnetic materials is the temperature behavior of their magnetic susceptibility, which reveals a kink at a certain temperature T_f (the freezing temperature) whose shape and position depend on the magnitude

() email: gorshunov@ran.gpi.ru

and alternation frequency of the probing field [3]. Spin glasses possess magnetic memory: the magnitude of magnetization created by an external magnetic field below T_f depends on the pre-history of the system. Typical for a spin-glass state are relaxational phenomena with characteristic times which at low temperatures can by far exceed the duration of the experiment. In spite of the large number of theoretical and experimental investigations, there is still no generally accepted consensus on the nature of the spin-glass state and the majority of properties of spin glasses remain not fully understood [1,3{5].

Since the RKKY interaction plays a fundamental role in the physics of spin glasses, the behavior of the subsystem of free electrons should be intimately linked to the formation and stabilization of the spin-glass phase. The magnitude of the RKKY interaction depends on the electronic mean free path, as was first shown by de Gennes [6]. Thus, investigating the characteristics of conduction electrons gives insight into the peculiar physics of spin glasses. The most direct way to study the properties of delocalized electrons is provided by electrical transport experiments. Immediately following the first works on spin glasses, the electrical resistance of "classical" systems like AuFe, CuMn, AuMn, and AuCr has been investigated in a detailed and systematic way as a function of temperature, magnetic field and concentration of magnetic centers [7{11]. It was shown that the magnetic contribution to the electrical resistivity (ρ) reveals a $T^{3=2}$ temperature dependence at the lowest temperatures and a T^2 dependence close to T_f ; at elevated temperatures $T > T_f$ there is a broad maximum in (ρ) which is due to a competition between Kondo and RKKY interactions in the subsystems of electrons and magnetic moments. Existing theories encounter serious difficulties to reproduce the temperature behavior of the resistivity in broad intervals of temperatures and impurity concentrations [3]. Certain difficulties are also caused by deviations from Matthiessen's rule at elevated temperatures.

Fundamental information on the properties of the electronic subsystem can be obtained by optical spectroscopy, which for instance allows one to extract such characteristics of free carriers as mechanisms of scattering and relaxation, energy gaps and pseudogaps in the density of states, localization and hopping parameters, size and granularity effects in thin conducting films [12]. However, to our knowledge, there are no data published on optical spectroscopy of spin glasses. The reason may be purely technical: since these materials are highly conducting, almost like regular metals, it is practically impossible to measure their electrodynamic properties by standard spectroscopical techniques, especially in the far-infrared range and at even lower frequencies where effects of interactions of mobile electrons with localized spins and between these spins should reveal themselves. Here we present the first measurements of the electrodynamic response of the spin-glass compound AuFe in a broad range of frequencies with an emphasis on the THz range corresponding to energies of the radiation quanta which are close to the RKKY binding energy.

Experimental Techniques. { For the measurements we have chosen the well-studied spin-glass compound AuFe. A set of films with different thicknesses and Fe concentrations was prepared. The high purity metals were co-sputtered onto a high-resistive Si substrate (size $10 \times 10 \text{ mm}^2$, thickness about 0.5 mm). Before the argon sputter gas was admitted the equipment was pumped down to UHV conditions (10^{-7} torr) to prevent oxidation of the films during fabrication. The films were analyzed using Rutherford backscattering and electron microprobe analysis; the thickness and composition was homogeneous. In this paper we concentrate on the results obtained for an AuFe film with 6 at.% of Fe and about 50 nm thickness. We also measured a pure Au film of the same thickness prepared under the same conditions.

For the THz investigations a coherent source spectrometer [13] was used which operates

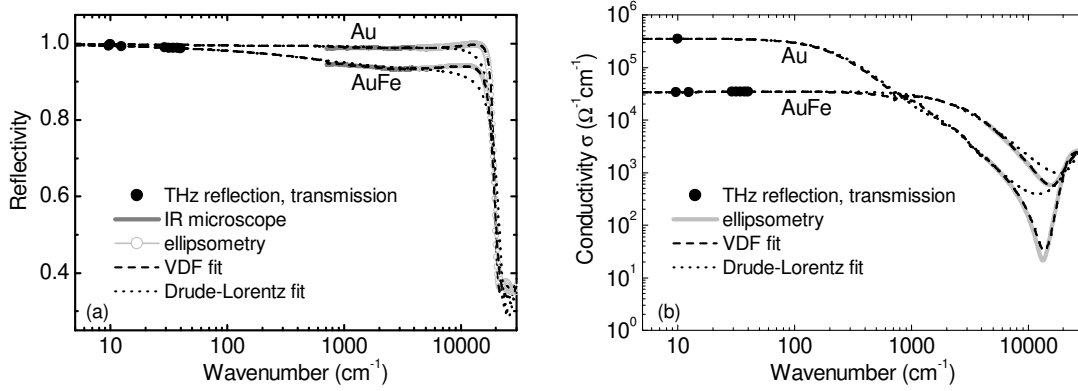


Fig.1 { (a) Room temperature reflectivity and (b) conductivity of Au and AuFe (6 at.% Fe) in s. The full circles below 50 cm^{-1} are from THz transmission and reflection measurements. The solid curves correspond to the IR reflection measurements. The reflectivity calculated from the ellipsometric measurements is given by grey open circles and lines. The thick lines in the conductivity spectra between 5000 cm^{-1} and 33000 cm^{-1} are directly calculated from ellipsometric data. The dotted lines are the fits by a simple Drude-Lorentz model. The dashed lines indicate a combined fit of reflectivity and conductivity by an advanced Drude-Lorentz model based on the variational dielectric function introduced in [17].

in the frequency range from 30 GHz up to 1.5 THz ($1 - 50 \text{ cm}^{-1}$). This range is covered by a set of backward-wave oscillators as powerful sources of radiation whose frequency can be continuously tuned within certain limits. In a quasioptical arrangement the complex (amplitude and phase) transmission and reflection coefficients can be measured at temperatures from 2 K to 1000 K and in a magnetic field up to 8 Tesla if required. Dynamical conductivity of Au and AuFe in s was directly determined from THz transmissivity and reflectivity spectra in a way we have used for measurements on other conducting in s, like heavy fermions [14] or superconductors [15].

In order to complete our overall picture, the samples were optically characterized up to the ultraviolet. The room temperature experiments were conducted on the same Au and AuFe in s as the THz investigations. In the infrared spectral range ($600 - 7000 \text{ cm}^{-1}$), optical reflectivity $R(\omega)$ measurements were performed using an infrared microscope connected to a Bruker IFS 66v Fourier transform spectrometer. An aluminum mirror served as reference, whose reflectivity was corrected by the literature data [16]. A Woollam vertical variable angle spectroscopic ellipsometer (VASE) equipped with a Berek compensator was utilized to measure in the energy range between 5000 cm^{-1} and 33000 cm^{-1} with a resolution of 200 cm^{-1} under multiple angles of incident between 65° and 85° . From the ellipsometric measurements we obtain the real and imaginary parts of the refractive index which then allow us to directly evaluate any optical parameter like the reflectivity $R(\omega)$ or the conductivity $\sigma(\omega)$.

Experimental Results and Discussion. { To analyze the frequency dependent transport, we first consider the room temperature results displayed in Fig.1. It is seen that the spectra for both Au and AuFe are metallic [12]: the reflectivity reveals a characteristic plasma edge around 20000 cm^{-1} and the conductivity $\sigma(\omega)$ is only weakly frequency dependent at low frequencies and quickly drops between 10^3 cm^{-1} and 10^4 cm^{-1} . The increase of the conductivity at even higher frequencies (above $2 \cdot 10^4 \text{ cm}^{-1}$) is caused by electronic interband transitions. In order to extract the microscopic characteristics of charge carriers, we fitted the spectra

Table I { Drude parameters of the free charge carriers in Au and AuFe (6 at.% Fe) films obtained by a Drude-Lorentz fit to the room temperature spectra of Fig. 1 with the dc ($\omega \rightarrow 0$) conductivity σ_{dc} , the scattering rate γ , scattering time τ , and the plasma frequency $\omega_p = \sqrt{4\pi n e^2/m}$ with n and e being the concentration and the charge of the carriers, and m their effective mass.

Film	σ_{dc} ($\Omega^{-1} \text{cm}^{-1}$)	γ (cm^{-1})	τ (s)	ω_p (cm^{-1})
Au	350 500	236	$2.25 \cdot 10^{-14}$	70 450
AuFe	33 600	2445	$2.17 \cdot 10^{-15}$	70 100

by the Drude model of conductivity [12]: $\sigma(\omega) = \sigma_{dc}/(1 - i\omega\tau)$, where σ_{dc} denotes the dc conductivity and $\tau = 1/(2\gamma)$ the relaxation time and γ the relaxation rate of charge carriers (c is the speed of light). The higher frequency interband transitions were roughly modelled by additional Lorentz oscillators. The results of the fit are presented by dashed lines in Fig. 1, the parameters are summarized in Table I. As indicated by the dotted lines, both the reactivity and conductivity spectra can be perfectly reproduced by a more advanced procedure based on the variational analysis of the optical reactivity and conductivity spectra introduced by Kuzmenko [17]. The low-frequency conductivity is smaller and the scattering rate of carriers larger (more than ten times) in AuFe compared to Au. Obviously, the differences should be ascribed to additional magnetic scattering of electrons in AuFe. Although the plasma frequency is not affected when Fe is diluted in Au, the distribution of spectral weight (as measured by the center of gravity, for instance) is shifted to higher energies.

The temperature dependence of the transport characteristics is presented in Fig. 2. The upper panel compares the ac resistivity ($\rho(\omega) = 1/\sigma(\omega)$) of the AuFe (6 at.% Fe) and Au films

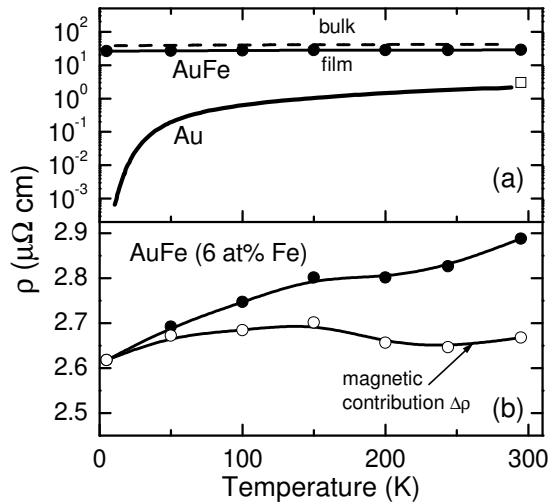


Fig. 2 { (a) Temperature dependent ac and dc resistivities of Au and AuFe. The solid dots correspond to ac resistivity ($\rho(\omega) = 1/\sigma(\omega)$) of AuFe film (6 at.% Fe) measured at 35 cm^{-1} (1.05 THz). The dashed line refers to the dc resistivity obtained for bulk AuFe with 5 at.% of Fe [9]. The solid line indicates the dc resistivity of bulk gold [9]. The square shows the ac resistivity of Au film at 35 cm^{-1} (1.05 THz). (b) The temperature dependence of the magnetic contribution to the ac resistivity evaluated by $\rho(T) = \rho_{\text{AuFe}}(T) - \rho_{\text{Au}}(T)$ is shown by the open circles; for comparison the ac resistivity of the AuFe film is re-plotted on a linear scale (solid dots).

to the dc resistivity of a bulk AuFe (with slightly different Fe concentration of 5 at.%) and of pure bulk Au samples (data from Ref. [9]).

First, it is obvious that at all temperatures the resistivity of our AuFe film is very close to that of the bulk material: for example, at room temperature $\rho_{\text{AuFe}}(\text{film}) \approx 30 \text{ m}\Omega$ and $\rho_{\text{AuFe}}(\text{bulk}) \approx 40 \text{ m}\Omega$. The same holds for the pure Au samples: $\rho_{\text{Au}}(\text{film}) \approx 3 \text{ m}\Omega$ and $\rho_{\text{Au}}(\text{bulk}) \approx 2 \text{ m}\Omega$. This agreement indicates the very good quality of our thin films and that there are basically no effects on their ac electrical properties connected with a possible granular structure. The same conclusion is also drawn from the measurements of the freezing temperatures $T_f \approx 25 \text{ K}$ of our AuFe film which appears to be basically the same as those for bulk samples.

Furthermore, it is seen from Fig. 2 that at all temperatures the resistivity of AuFe is much larger than the resistivity of Au; the difference increases when cooling down. This is a consequence of scattering of the charge carriers on magnetic impurities that prevails over phonon scattering in the entire temperature range. The resistivity $\rho(T)$ reveals a broad feature around 100–150 K which is ascribed to the interplay of Kondo and RKKY regimes [8,11]. At high temperatures thermal excitations exceed the RKKY energy of interacting impurities and a Kondo-like scattering of electrons on independent magnetic moments dominates. This leads to a weak increase of the magnetic contribution to the resistivity ρ_{mag} upon cooling as demonstrated by the open circles in Fig. 2b where the difference $\rho = \rho_{\text{AuFe}} - \rho_{\text{Au}} = \rho_{\text{mag}}$ is plotted. At low temperatures the RKKY interaction between magnetic moments starts to sum up and causes a noticeable suppression of the magnetic contribution to the resistivity. Assuming Matthiessen's rule [18], the scattering rate of electrons due to magnetic interaction in AuFe at $T = 300 \text{ K}$ can be calculated as $\rho_{\text{mag}} = \rho_{\text{AuFe}} - \rho_{\text{Au}} \approx 2210 \text{ m}\Omega$.

In the low temperature regime, also the frequency dependent conductivity of AuFe is distinct from the room temperature behavior as demonstrated in Fig. 3 where the THz spectra of $\sigma(\omega)$ for AuFe are presented. Above approximately 100 K, $\sigma(\omega)$ is basically frequency independent in accordance with the Drude model which predicts a constant conductivity for

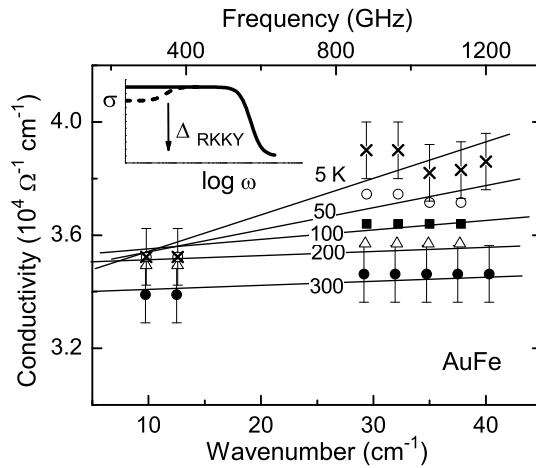


Fig. 3 { Terahertz conductivity spectra of the AuFe film (6 at.% Fe) at various temperatures. For $T < 100 \text{ K}$ a positive dispersion indicates localization effects. The lines are guides to the eye. The inset shows schematically how the Drude-like conductivity spectrum of free electrons (solid line) is modified by a gap-like structure (dashed line) due to the RKKY interaction between Fe magnetic moments mediated by these electrons.

frequencies much smaller than the scattering rate [12], as sketched in the inset of Fig. 3 by the solid line; the scattering rate for AuFe equals 2445 cm^{-1} at 300 K (Table I), i.e., far above the range of frequencies presented in Fig. 3. This changes drastically for $T < 100 \text{ K}$, when the conductivity (σ) increases towards high frequencies. We associate this conductivity dispersion with a pseudogap which appears in the free electron excitations when the RKKY interaction between Fe centers mediated by the conduction electrons sets in. In a simple picture the electrons which participate in the RKKY interaction can be regarded as being to some extent bound to (or localized between) the corresponding pairs of magnetic moments, as long as the thermal energy $k_B T$ does not exceed this "binding energy" which should be of order of the RKKY interaction J_{RKKY} . This will lead to a corresponding reduction of the dc conductivity and also of the ac conductivity for frequencies below $J_{\text{RKKY}} = \hbar$. At higher frequencies, $\omega > J_{\text{RKKY}} = \hbar$, the electrons will no longer be affected (and localized) by the RKKY interaction and hence the conductivity (σ) should increase around $J_{\text{RKKY}} = \hbar$ to approach the unperturbed value. In other words, one would expect a gap-like feature to appear in the conductivity spectrum, as depicted by the dashed line in the inset of Fig. 3. The RKKY energy is approximately given by the freezing temperature T_f [19], which for AuFe (6 at.% of Fe) is about 25 K [9,20], yielding $J_{\text{RKKY}} = k_B T_f = 2.2 \text{ meV}$. For the characteristic frequency we then obtain $J_{\text{RKKY}} = \hbar = 17 \text{ cm}^{-1}$ (510 GHz). This falls just in the range where the dispersion of the conductivity of AuFe in the spin-glass state is observed. The effect amounts to approximately 10%, meaning that about one tenth of the conduction electrons participate in the RKKY interaction.

According to our picture of spin-glass systems, the conduction electrons experience two effects from the RKKY interaction mediated by these electrons. On one hand, a decrease of the resistivity is commonly observed while cooling below T_f because the RKKY correlations between magnetic moments progressively suppress the Kondo-type scattering. On the other hand, a certain fraction of carriers is increasingly bound to the magnetic moments by participating in the RKKY interaction and is thus taken out of the conduction channel. The competing character of the two effects is clearly seen in Fig. 3: while cooling down, the gap-like feature appears on top of a background conductivity which increases basically at all shown frequencies. In order to verify our assumptions, a comprehensive study is required on various spin-glass materials with different freezing temperature and consequently different J_{RKKY} .

Conclusions. { The optical spectra of pure gold and spin glass AuFe (6 at.% Fe) films have been investigated in a broad frequency range from 10 cm^{-1} up to 33000 cm^{-1} using three different spectroscopic techniques. At ambient temperature the microscopic charge-carrier parameters in pure gold and in AuFe are determined. For the spin glass AuFe the scattering rate of the carriers is significantly enlarged due to their interaction with localized magnetic moments. At reduced temperatures ($T < 100 \text{ K}$) when the RKKY interaction gains importance as the spin-glass state is formed, a pseudogap feature in the optical conductivity spectrum is detected of a magnitude close to the RKKY energy in AuFe. We associate the origin of the pseudogap with partial localization of those electrons which are involved in the RKKY interaction between magnetic moments.

Acknowledgements. { The work was supported by the Russian foundation for Basic Research, grant N 06-02-16010-a and the Deutsche Forschungsgemeinschaft (DFG). We also thank the Foundation for Fundamental Research of Matter (FOM).

- [1] A.M.Ydosh, Spin glasses: an experimental introduction, (Taylor and Francis, London, 1993); Spin glasses and random fields, edited by A.P.Young (World Scientific, Singapore, 1997).
- [2] A.J.Freeman, in: Magnetic Properties of Rare Earth Metals edited by R.J.Elliott (Plenum, London, 1972).
- [3] K.Binder and A.P.Young, Rev.Mod.Phys. 58, 801 (1986).
- [4] K.H.Fischer and J.A.Hertz, Spin glasses (Cambridge University Press, Cambridge, 1991).
- [5] M.Mezard, G.Parisi, M.A.Virasoro, Spin Glass Theory and Beyond (World Scientific, Singapore, 1987).
- [6] P.G.deGennes, J.Phys.Radium 23, 630 (1962).
- [7] J.W.Loram, T.E.Whall, and P.J.Ford, Phys.Rev.B 2, 857 (1970).
- [8] P.J.Ford, T.E.Whall, and J.W.Loram, Phys.Rev.B 2, 1547 (1970).
- [9] J.A.Mydosh, P.J.Ford, M.P.Kawatra, and T.E.Whall, Phys.Rev.B 10, 2845 (1974).
- [10] P.J.Ford and J.A.Mydosh, Phys.Rev.B 14, 2057 (1976).
- [11] I.A.Campbell, P.J.Ford, and A.Hamzic, Phys.Rev.B 26, 5195 (1982).
- [12] M.Dressel and G.Gruner, Electrodynamics of Solids (Cambridge University Press, Cambridge, 2002).
- [13] A.A.Volkov, Yu.G.Goncharov, G.V.Kozlov, S.P.Lebedev, and A.M.Prokhorov, Infrared Phys. 25, 369 (1985); A.A.Volkov, G.V.Kozlov, and A.M.Prokhorov, Infrared Phys. 29, 747 (1989); G.Kozlov, A.Volkov, Coherent Source Submillimeter Wave Spectroscopy, in: Millimeter and Submillimeter Wave Spectroscopy of Solids, edited by G.Gruner (Springer, Berlin, 1998), p. 51; B.Gorshunov, A.Volkov, I.Spektor, A.Prokhorov, A.Mukhin, M.Dressel, S.Uchida, and A.Loidl, Int.J.of Infrared and Millimeter Waves, 26, 1217 (2005).
- [14] M.Dressel, N.V.Kasper, B.Gorshunov, K.Petukhov, D.N.Peligrad, M.Jourdan, M.Huth, and H.Adrian, Phys.Rev.B 66, 035110 (2002)
- [15] A.V.Pronin, B.P.Gorshunov, A.A.Volkov, G.V.Kozlov, N.P.Shabanova, S.I.Krasnosvobodtsev, V.S.Nozdrin, and E.V.Pechen, JETP 82, 790 (1996); A.V.Pronin, M.Dressel, A.Pimenov, A.Loidl, I.Roshchin, and L.H.Greene, Phys.Rev.B 57, 14416 (1998).
- [16] Handbook of Optical Constants of Solids, Vol. I, edited by E.D.Palik, (Academic Press, Orlando, 1985).
- [17] A.B.Kuzmenko, Rev.Sci.Instrum. 76, 083108 (2005); <http://optics.unige.ch/alexey/re.html>
- [18] J.Bass, Adv.Phys. 21, 431 (1972).
- [19] J.S.Schilling, P.J.Ford, U.Larsen, and J.A.Mydosh, Phys.Rev.B 14, 4368 (1976).
- [20] V.Canella and J.A.Mydosh, Phys.Rev.B 6, 4220 (1972).